The Plant Cell, Vol. 20: 1482–1493, June 2008, www.plantcell.org © 2008 American Society of Plant Biologists

Mutation of *Arabidopsis BARD1* Causes Meristem Defects by Failing to Confine *WUSCHEL* Expression to the Organizing Center [W] [OA]

Pei Han,[a,1] Qing Li,[a,1] and Yu-Xian Zhu[a,b,c,2]

[a] National Laboratory of Protein Engineering and Plant Genetic Engineering, College of Life Sciences, Peking University, Beijing 100871, China

[b] National Center for Plant Gene Research, Beijing 100101, China

[c] Peking-Yale Joint Center for Plant Molecular Genetics and Agrobiotechnology, College of Life Sciences, Peking University, Beijing 100871, China

Stem cell fate in the *Arabidopsis thaliana* shoot apical meristem (SAM) is controlled by *WUSCHEL* (*WUS*) and *CLAVATA*. Here, we examine BARD1 (for BRCA1-associated RING domain 1), which had previously been implicated in DNA repair functions; we find that it also regulates WUS expression. We observed severe SAM defects in the knockout mutant *bard1-3*. *WUS* transcripts accumulated >238-fold in *bard1-3* compared with the wild type and were located mainly in the outermost cell layers instead of the usual organizing center. A specific *WUS* promoter region was recognized by nuclear protein extracts obtained from wild-type plants, and this protein-DNA complex was recognized by antibodies against BARD1. The double mutant (*wus-1 bard1-3*) showed prematurely terminated SAM structures identical to those of *wus-1*, indicating that BARD1 functions through regulation of WUS. *BARD1* overexpression resulted in reduced *WUS* transcript levels, giving a *wus-1*–like phenotype. Either full-length *BARD1* or a clone that encoded the C-terminal domain (BARD1:C-ter;*bard1-3*) was sufficient to complement the *bard1-3* phenotype, indicating that BARD1 functions through its C-terminal domain. Our data suggest that *BARD1* regulates SAM organization and maintenance by limiting *WUS* expression to the organizing center.

INTRODUCTION

The ability of flowering plants to continuously produce new organs depends on the activity of stem cell pools, which are located close to the tip of the meristem (Mayer et al., 1998). *WUSCHEL* (*WUS*) is a key gene involved in positioning the stem cells and is essential for organization and maintenance of the shoot apical meristem (SAM) (Laux et al., 1996; Schoof et al., 2000; Muller et al., 2006). In *Arabidopsis thaliana*, activation of the *CLAVATA3* (*CLV3*)–dependent signaling pathway reduces the rate of stem cell proliferation and enhances organ initiation via a feedback loop that inhibits *WUS* expression (Clark et al., 1997; Brand et al., 2000; Schoof et al., 2000; Muller et al., 2006). Ectopic expression of a *WUS* transgene in *Arabidopsis* induces shoot stem cell activity in root and floral meristems on the mature stem surface (Gallois et al., 2004; Xu et al., 2005). Transgenic *Arabidopsis* plants expressing a cauliflower mosaic virus 35S promoter (*CaMV35S*)*::WUS* construct showed severe growth inhibition and substantially reduced cotyledon expansion and greening (Brand et al., 2002; Lenhard et al., 2002; Kieffer et al., 2006). A similar interaction between *WUS* and *AGAMOUS* operates during *Arabidopsis* flower development (Lenhard et al., 2001; Lohmann et al., 2001). Recently, *WUSCHEL-RELATED HOMEOBOX5* (*WOX5*), a homolog of *WUS* that is expressed specifically in the quiescent center of the root, was found to serve as the root stem cell organizer (Sarkar et al., 2007).

WUS might function as a repressor of transcription in concert with the groucho-type corepressor protein TOPLESS (TPL), which functions by recruiting gene silencing machinery such as histone deacetylase 19 (Long et al., 2006). The C-terminal domain of both *Arabidopsis* WUS and its *Antirrhinum majus* ortholog ROSULATA binds the TPL protein (Kieffer et al., 2006). In the *Arabidopsis tpl-1* mutant, the embryonic shoot apex is transformed into a second root pole, and *WUS* is expressed normally until globular-stage embryos but is totally absent in the transition stage that produces two root axes (Long et al., 2006). In the *Arabidopsis* mutant *l28*, in which *WUS* and *CLV3* expression is abolished as the result of a mutation in the transcription factor *APETALA2*, the shoot meristem was prematurely terminated (Wurschum et al., 2006). Expression of *HANABA TARANU*, which encodes a GATA-3–like transcription factor, in vascular tissues and cells separating the meristem from organ primordia controls the number and the correct positioning of *WUS*-expressing cells (Zhao et al., 2004; Tucker and Laux, 2007).

Upon execution of a large-scale promoter scanning experiment, Baurle and Laux (2005) found that a 57-bp *cis*-element including an HD-ZIP consensus binding site–like motif located in

[1] These authors contributed equally to this work.

[2] Address correspondence to zhuyx@water.pku.edu.cn.

The author responsible for distribution of materials integral to the findings presented in this article in accordance with the policy described in the Instructions for Authors (www.plantcell.org) is: Yu-Xian Zhu (zhuyx@water.pku.edu.cn).

[W] Online version contains Web-only data.

[OA] Open Access articles can be viewed online without a subscription.

www.plantcell.org/cgi/doi/10.1105/tpc.108.058867

the distal (−530 to −586) promoter region of the *WUS* gene provides all the spatial and temporal information necessary for WUS transcription in the stem cell niche. *WUS* transcription is also modulated through direct binding of SPLAYED (SYD), a SNF2 chromatin-remodeling ATPase, to its proximal (−435 to −70) promoter region. In a chromatin immunoprecipitation assay that used polyclonal antibodies raised against the N-terminal domain of SYD, this proximal region was highly represented, but a distal region (−1664 to −1348) and the transcribed region were not (Kwon et al., 2005).

BARD1 (At1g04020) encodes a protein containing two tandem BRCA1 C-Terminal (BRCT) domains, which function in phosphorylation-dependent protein–protein interactions (Glover et al., 2004; Narod and Foulkes, 2004; Williams et al., 2004), and a RING domain, and it is located on *Arabidopsis* chromosome 1; *BARD1* reportedly is involved in DNA repair (Reidt et al., 2006). A similar gene on chromosome 4 (At4g21070) with almost identical BRCT and RING domain structures was named At *BRCA1* after the original human breast cancer–associated gene 1 (*BRCA1*) (Lafarge and Montane, 2003). Human BRCA1 and BARD1, the BRCA1-associated ring domain 1 protein, can form heterodimers through their common N-terminal RING domains and together function as tumor suppressors. These proteins have been implicated in many processes, including cell cycle control, DNA repair, recombination, and transcriptional regulation (Wu et al., 1996; Baer and Ludwig, 2002; Irminger-Finger and Jefford, 2006). BARD1 is indispensable for cell viability in mammals because loss-of-function mutations result in early embryonic lethality (Irminger-Finger and Jefford, 2006). To elucidate the mode of BARD1 function in *Arabidopsis*, we obtained all three T-DNA insertion lines that disrupted its expression from the SALK collections. Here, we provide molecular and genetic evidence to show that *BARD1* mutations cause severe SAM defects in *Arabidopsis* by releasing *WUS* expression from its normal confinement to the organizing center (OC), allowing its expression to spread to the outermost cell layers in the SAM.

RESULTS

Identification of Homozygous *BARD1* Knockout Mutant Lines

Three *Arabidopsis* mutant lines with disrupted *BARD1* were obtained from the SALK collection; T-DNA insertions were found in the first intron and in the third exon (SALK_097601 and SALK_031862 lines or *bard1-1* and *bard1-2*, respectively) and also in the last exon (SALK_003498 line or *bard1-3*) (see Supplemental Figure 1A online). We identified plants homozygous for *bard1-3*, with a single T-DNA insertion that completely blocked *BARD1* expression (see Supplemental Figures 1B to 1D online). Confirming that the phenotype is specific to the *BARD1* locus, RT-PCR analysis did not reveal a significant shift in the expression pattern of 10 putative open reading frames (ORFs) located adjacent to *BARD1* on the chromosome, either upstream or downstream of the *bard1-3* mutation (see Supplemental Figure 1E online). Because the *bard1-1* and *bard1-2* alleles had previously been implicated in DNA repair (Reidt et al., 2006), we tested *bard1-3* for the phenotype. The UV-C recovery assay (see Supplemental Figure 2A online) and terminal transferase dUTP nick end labeling (TUNEL)–based in situ cell death analysis (see Supplemental Figure 2B online) revealed obvious defects in DNA repair in *bard1-3* seedlings.

Phenotypic Characterization of the *bard1-3* Mutant

Severe developmental defects in plant architecture, especially in SAM organization, were observed in homozygous *bard1-3* seedlings (Figure 1). At 5 d after germination (DAG), SAMs of the wild type and mutant were not fundamentally different, except that the apical tissue of *bard1-3* was somewhat enlarged (Figures 1A to 1D). Significant differences were observed in seedlings at 7 DAG or older. Instead of the well-organized tunica-corpus structure observed in wild-type sections (Figures 1F and 1J), one or more irregular primordia with compact and presumably actively dividing cell populations was observed in mutant apical tissue, as indicated by condensed toluidine blue staining (Figures 1H and 1L). Also, in contrast with wild-type leaves (Figure 1N), a large number of tubular and finger-like structures was produced on the mutant (Figures 1O and 1P), indicating that proper BARD1 function is required for the development of leaf dorsoventrality in *Arabidopsis*.

In the *bard1-3* mutant, the elongation growth of primary roots, but not root hairs, was also significantly inhibited (see Supplemental Figure 3C online and the wild type in Supplemental Figure 3A online). Similar to what was observed in the SAM of the mutant, its root apical meristem and all the lateral root meristems were significantly enlarged, with huge cell masses (see Supplemental Figures 3E and 3G online). Lugol's staining (Sarkar et al., 2007) revealed that no starch granules and no columella cells were present in the root tips of the mutant (see Supplemental Figures 3B and 3D online), while 4′,6-diamidino-2-phenylindole (DAPI) staining showed the existence of large quantities of undifferentiated cells in the meristems (see Supplemental Figures 3F and 3H online). These results indicated that the *bard1-3* mutation affected the development of both the SAM and the root apical meristem during the embryo stage.

Identification of *WUS* as a Molecular Target of *BARD1*

To determine the molecular target of *BARD1*, we searched the Genevestigator database (Zimmermann et al., 2004) and looked for genes that were specifically expressed in the same proliferating cell types as *BARD1*. A total of 25 genes showed expression ratios >10 (comparing transcript level in dividing tissues, either shoot apex, embryo, or radicles, to ground tissues, either leaves, stems, or roots). Extensive RT-PCR analyses showed that, of the whole set of candidate genes, *WUS* was the most significantly upregulated in the *bard1-3* background (see Supplemental Figure 4A online). *STM*, *CLV3*, *WOX2*, *WOX5*, and *CUC1* expression was also significantly, but not as dramatically, upregulated in the mutant (see Supplemental Figure 4A online). Quantitative RT-PCR (QRT-PCR) data, represented as fold changes relative to the wild-type values, are reported beneath the respective RT-PCR data for those candidate genes that showed significantly different transcript levels in the mutant by visual inspection (see Supplemental Figure 4A online). Wild-type levels of *BARD1* transcripts were found in the *wus-1* mutant (see

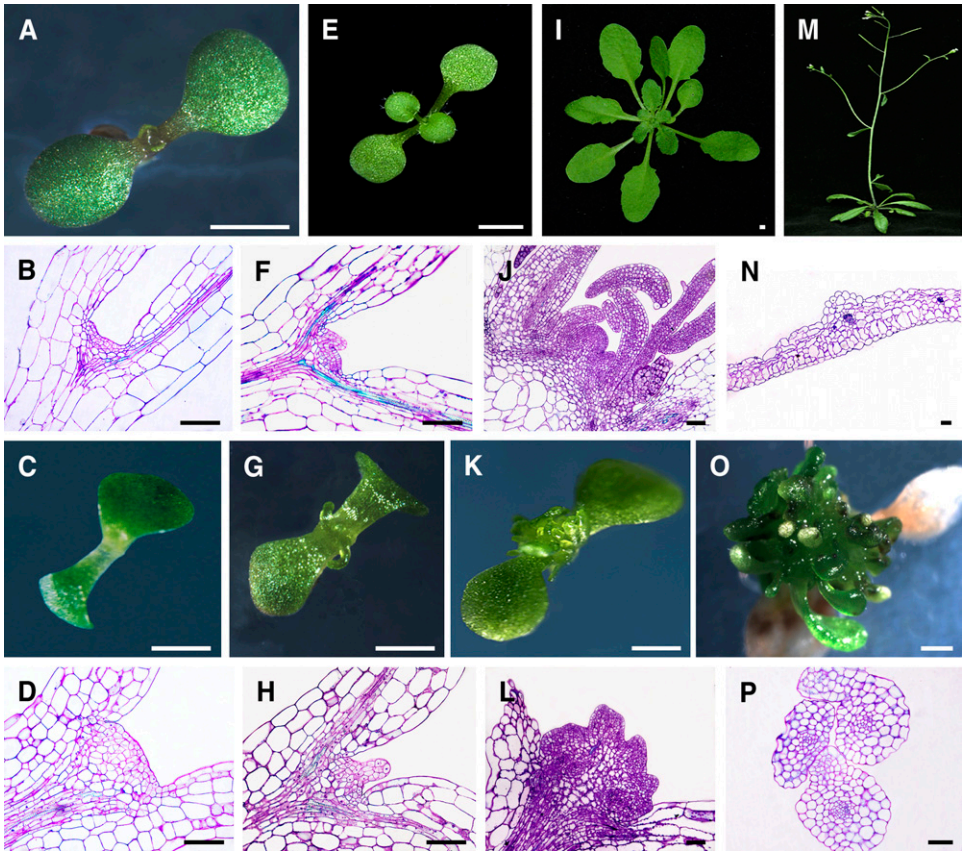

Figure 1. Phenotypic Characterization of the *bard1-3 Arabidopsis* Mutant.

Wild-type Columbia (Col-0) plants are shown in the top two rows, and *bard1-3* plants are shown in the bottom two rows. **(A)**, **(E)**, **(I)**, and **(M)** were photographed at the same growth period with panels **(C)**, **(G)**, **(K)**, and **(O)**, respectively. White bars = 1 mm; black bars = 50 μm.
(A) to **(D)** Seedlings 5 DAG.
(E) to **(H)** One-week-old seedlings.
(I) to **(L)** Three-week-old plants.
(M) and **(O)** Five-week-old plants.
(A), **(E)**, **(I)**, and **(M)** Photographs of wild-type Col-0 plants.
(C), **(G)**, **(K)**, and **(O)** Photographs of the *bard1-3* mutant.
(B), **(F)**, and **(J)** Median longitudinal semithin sections stained with toluidine blue showing wild-type SAMs at corresponding growth stages.
(D), **(H)**, and **(I)** Sections of *bard1-3* mutant SAMs at growth stages described above.
(N) Cross section of a mature wild-type leaf.
(P) Cross section of the leaf-like structures from the 5-week-old *bard1-3* mutant.

Supplemental Figure 4B online), indicating that *WUS* does not regulate *BARD1* expression levels in *Arabidopsis*.

In Situ and QRT-PCR Analyses of *WUS* and *BARD1* Expression in Wild-Type and *bard1-3* Mutants

A series of in situ RNA hybridization experiments indicated that *BARD1* is expressed specifically in the apical domains of *Arabidopsis* inflorescence (Figure 2A), ovules (Figure 2B), anthers (Figure 2C), and embryos (Figure 2D). Hybridization results using a sense *BARD1* probe showed that the heavy staining in the surrounding seed coat of the developing embryo was not due to *BARD1* mRNA (Figure 2E). When very young seedlings were analyzed, *BARD1* transcripts localized mainly in the outermost three to four cell layers of the main shoot apex in wild-type seedlings and in developing leaf primordia and young leaves (Figure 3A), whereas *WUS* was localized specifically in the OC (Figure 3B). In *bard1-3* mutant seedlings, in which *BARD1* mRNA was not detectable (Figure 3C), a very strong *WUS* signal was observed in the outermost cell layers of multiple apical primordia–like structures (Figure 3D). QRT-PCR analysis using RNA samples prepared from whole young shoots indicated that *WUS* transcripts were 238.0 ± 12.3-fold higher (a difference of 9.31 ± 0.35 cycles) in the mutant relative to the wild type (Figure 3E).

The *BARD1* expression pattern was further studied by producing transgenic *Arabidopsis* plants that expressed a β-glucuronidase (*GUS*) construct driven by a 1.91-kb 5′ *BARD1* upstream promoter fragment (see Supplemental Figure 5 online). When

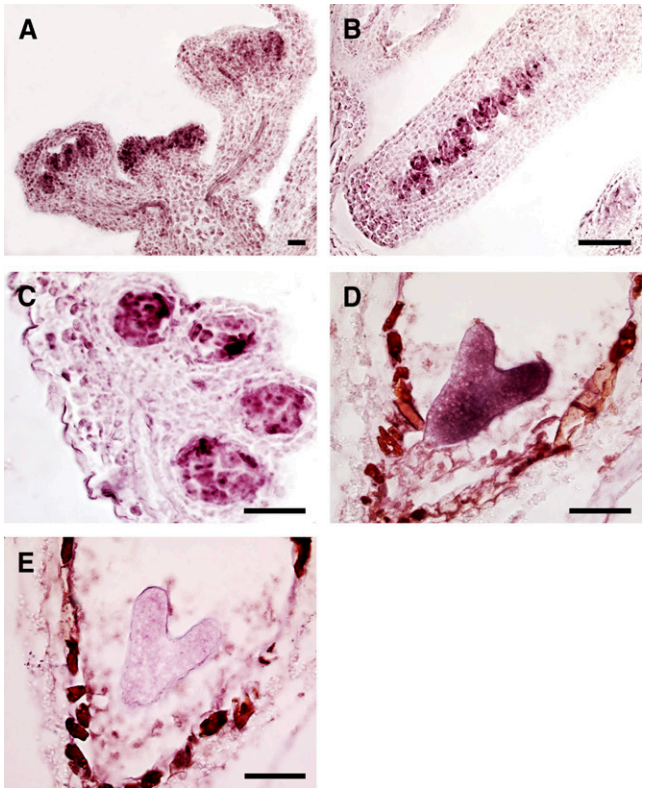

Figure 2. Tissue-Specific Expression of *BARD1* in Wild-Type *Arabidopsis* Plants.

In situ hybridization experiments using an antisense *BARD1* probe were performed on *Arabidopsis* inflorescence **(A)**, carpels **(B)**, anthers **(C)**, and the heart-shaped-stage embryo **(D)**. The same stage developing embryo shown in (D) was probed with a sense *BARD1* sequence **(E)** to demonstrate the specificity of our hybridization experiments. Bars = 50 μm.

cleared whole seedlings were assayed, strong GUS activity was observed in the shoot apex, including the developing leaf primordia (see Supplemental Figure 5A online). When longitudinal sections of *Arabidopsis* shoot apices were stained, GUS activity was localized mainly in the apical layers of the SAM (see Supplemental Figure 5B online), similar to the in situ hybridization results reported in Figure 3A. Strong GUS activity was also observed mainly in the meristem zone of primary roots (see Supplemental Figure 5C online) and in the initiation site of lateral roots (see Supplemental Figure 5D online). We also constructed a GUS construct driven by a fragment of the WUS promoter, but we were unable to produce *WUS:GUS* transgenic *Arabidopsis* on a *bard1-3* genetic background because the homozygous mutant was seedling lethal, and no *WUS:GUS bard1-3* seedlings were obtained even by a genetic cross using heterozygous *BARD1/bard1-3* plants.

BARD1 Is Involved in the Formation of a Protein-DNA Complex with Specific Regions on the *WUS* Promoter

Because BARD1 activity seemed to repress *WUS* expression, we used a gel shift assay to study possible molecular interactions between BARD1 and *WUS* using part of the *WUS* promoter (Kwon et al., 2005) as depicted in Figure 4A. Significant mobility shifts were observed when fragments 1 or 4 (F1 or F4) were incubated with wild-type nuclear extract (Figure 4B). The DNA-bound protein complex specifically appeared after the addition of nuclear extract prepared from wild-type *Arabidopsis* seedlings but not from *bard1-3* mutants (Figure 4C, lanes 2 and 4). Formation of the DNA-protein complex was blocked upon addition of specific unlabeled competitor probes but not when the nonspecific competitor poly(dI-dC) was added (Figure 4C, lanes 3 and 4), demonstrating sequence-specific binding. The protein-bound complex on F1 was most likely not related to BARD1 because similar binding was observed using wild-type or mutant nuclear extracts (Figure 4C, lanes 7 and 8). When a polyclonal antiserum to BARD1 was included in the binding reaction together with wild-type nuclear extract, another band with a higher

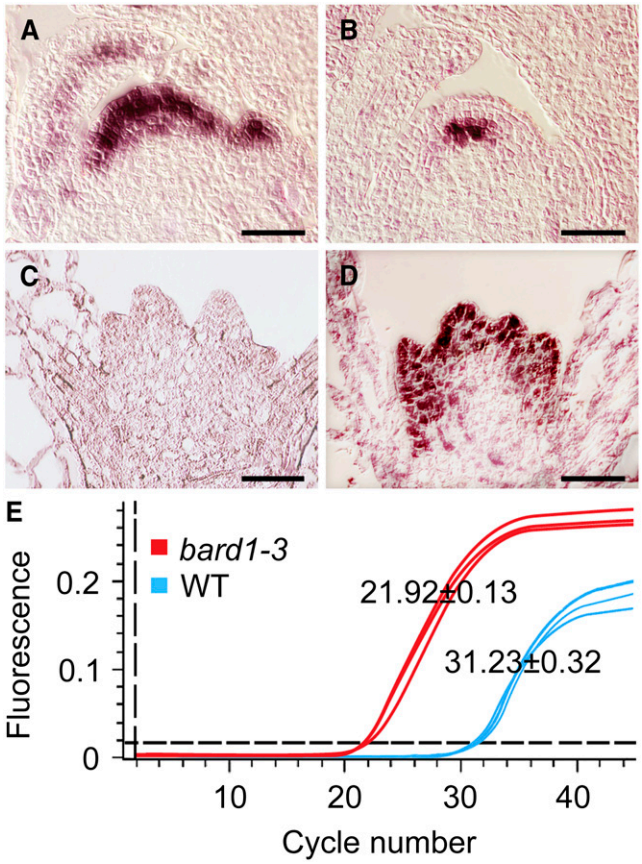

Figure 3. *WUS* Transcripts Are Detected in the Outermost Cell Layers, Instead of the Usual OC, in *bard1-3* SAMs.

(A) and **(B)** In situ hybridization of *BARD1* and *WUS*, respectively, in wild-type *Arabidopsis*.

(C) and **(D)** In situ hybridization of *BARD1* and *WUS*, respectively, in *bard1-3*. Bars = 20 μm.

(E) QRT-PCR analysis of *WUS* mRNA levels in the wild type and the *bard1-3* mutant. Mean (±SE) comparative threshold (CT) values were calculated from triplicate QRT-PCR experiments using independent RNA samples prepared from different batches of *Arabidopsis* plants.

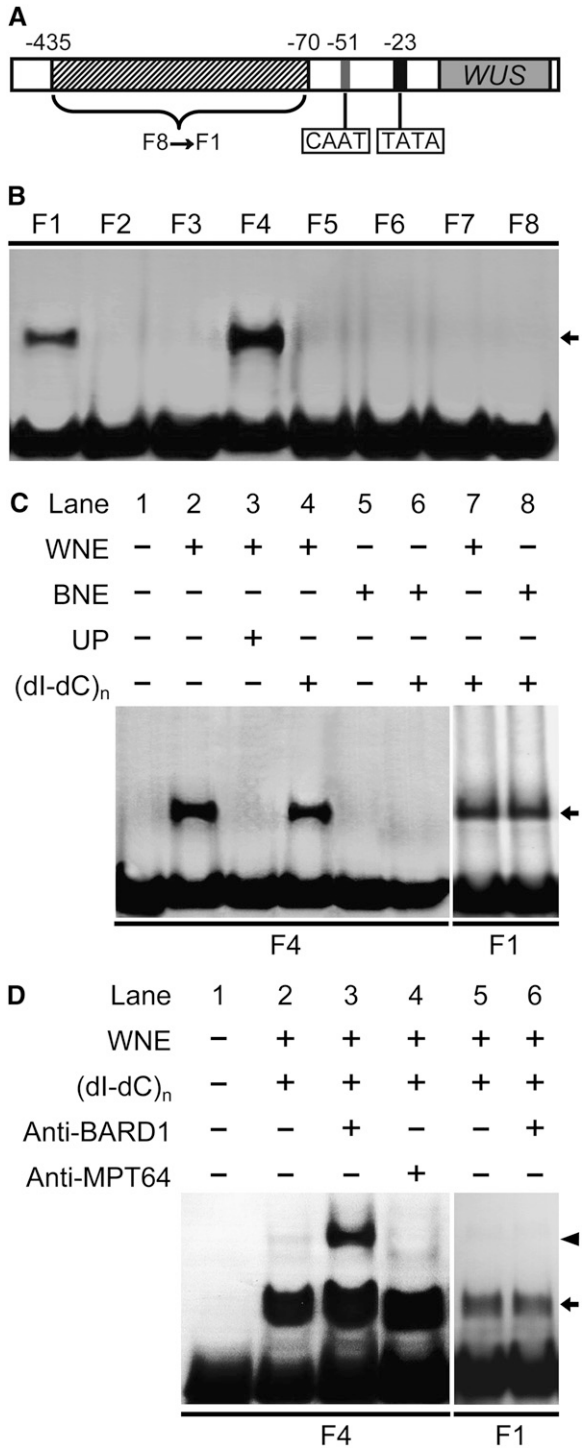

Figure 4. BARD1 Forms a Specific Complex on Fragment 4 of the *WUS* Promoter.

(A) Schematic diagram showing the *WUS* promoter region used for gel shift assays. Fragments: F1, −70 ~ −125; F2, −116 ~ −170; F3, −161 ~ −215; F4, −206 ~ −260; F5, −251 ~ –305; F6, −296 ~ −350; F7, −341 ~ −395; F8, −386 ~ −435 bp.

(B) Nuclear extracts prepared from wild-type plants form binding complexes with F1 and F4. The arrows in **(B)** to **(D)** indicate the DNA-protein complex.

molecular mass appeared (Figure 4D, lane 3), suggesting that BARD1 is part of the DNA-protein complex. This supershifted band was not observed when antiserum against a nonspecific bacterial protein was included (Figure 4D, lane 4). The complex on F1 did not react with anti-BARD1 (Figure 4D, lanes 5 and 6).

Truncated mRNAs Encoding Potentially Functional Polypeptides Are Found in Both *bard1-1* and *bard1-2* Mutants

To examine the differences between *bard1-1*/*bard1-2* and *bard1-3*, we performed detailed sequence analyses using genomic DNA from wild-type *Arabidopsis* plants. Putative ORFs were found in *bard1-1* and *bard1-2*, downstream of the T-DNA insertions (Figure 5A). We further sequenced the longest transcripts after repeated 5′ rapid amplification of cDNA ends (RACE) experiments using RNA templates from either *bard1-1* or *bard1-2* plants to find new potential transcription start sites (Figure 5A). The longest RNA from *bard1-1* included 19 nucleotides of the second intron at its 5′ end with all other intron sequences removed in the mature mRNA. The longest RNA from *bard1-2* started from the middle of the original exon 5 with no intron sequences attached (Figure 5A). Semithin sections of shoot meristems of *bard1-1* and *bard1-2* are shown in Figure 5B. Apart from the fact that both mutants were smaller and developed slower than the wild type, no other defects were observed. Full-length (2145 nucleotides) mRNA from the wild type and truncated mRNAs from *bard1-1* (2027 nucleotides) and *bard1-2* (1479 nucleotides) were successfully amplified, whereas no product was found in *bard1-3* using primer pairs derived either from the 5′ (1 to 485 nucleotides) or 3′ (1423 to 2145 nucleotides) regions for up to 35 PCR cycles (Figure 5C). QRT-PCR indicated that *bard1-1* and *bard1-2* mRNA levels were 39 and 46%, respectively, of the wild-type level (Figure 5D). No significant increase in *WUS* expression was detected in these two mutants, indicating that the C-terminal part of BARD1 is sufficient to repress *WUS* expression (Figure 5D).

Protein gel blotting experiments showed that our polyclonal antibody recognized BARD1 specifically because a single band with an apparent molecular mass similar to that calculated from the vector (79.7 kD for BARD1 + 2.6 kD for the tag) was observed in the lane containing total *Escherichia coli* protein after (+) but not before (–) isopropylthio-β-D-galactoside (IPTG) inductions (Figure 5E). One major band (apparent molecular mass of 52.5 kD) along with a weaker band (a presumptive degradation product of 43.4 kD) was observed for total protein prepared

(C) The DNA-bound protein complex on F4 only appears after adding wild-type nuclear extracts but does not form after adding bard1-3 extract. The protein complex on F1 is not specific. WNE, 10 μg wild-type nuclear extract; BNE, 10 μg *bard1-3* mutant nuclear extract; UP, 50-fold unlabeled probe; $(dI\text{-}dC)_n$, 0.5 μg poly(dI-dC).

(D) The protein-bound DNA complex on F4 is recognized by BARD1 antiserum, whereas that on F1 is not. Anti-BARD1, 20 nmol of polyclonal antibody against the C-terminal region of BARD1; anti-MPT64, 20 nmol of polyclonal antibody against MPT64 (Cai et al., 2005). The arrowhead indicates the DNA-protein-antibody complex.

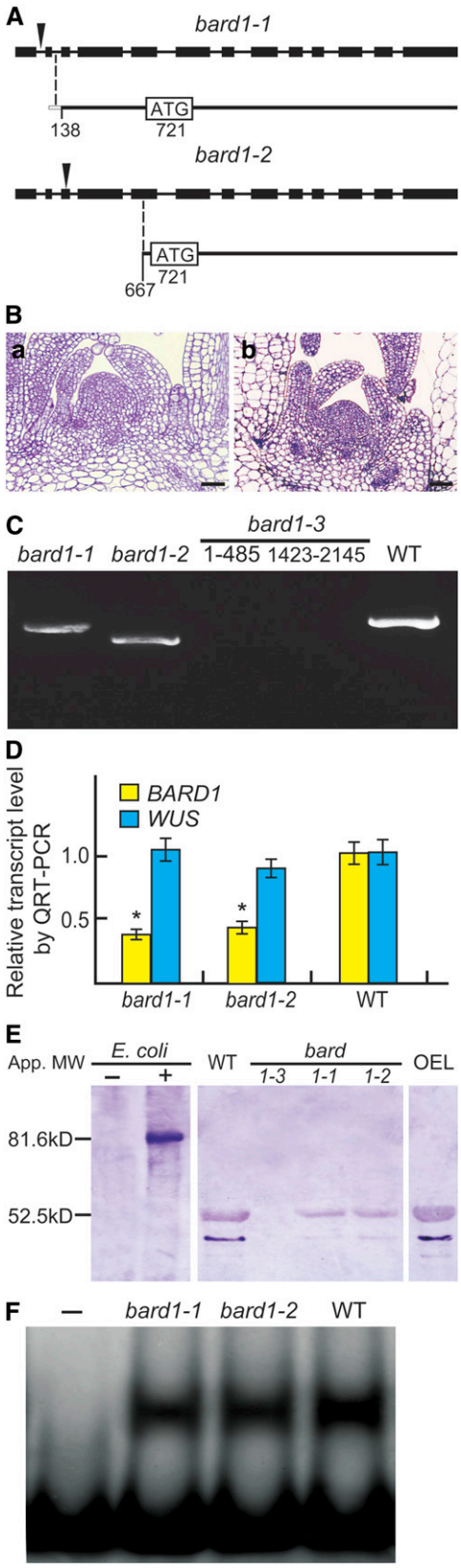

Figure 5. Molecular Analyses of Different Mutant Lines.

(A) Analysis of *bard1-1* and *bard1-2* transcripts. The 5′ RACE experiments were performed on RNA templates derived from *bard1-1* or *bard1-2*. Inverted triangles indicate the sites of the T-DNA insertions, black boxes denote exons, and the thin lines denote introns.

(B) Median longitudinal semithin sections stained with toluidine blue showing the SAMs of 3-week-old *bard1-1* (left) and *bard1-2* (right). Bars = 20 μm.

(C) RT-PCR analysis of *BARD1* RNAs. Full-length RNA from wild-type and truncated RNAs from *bard1-1* and *bard1-2* are shown. Two primer pairs derived from 5′ (1 to 485 nucleotides) and 3′ (1423 to 2145 nucleotides) regions were used to amplify *bard1-3*.

(D) Comparison of *WUS* and *BARD1* mRNA levels in wild-type, *bard1-1*, *1-2*, and *1-3* plants by QRT-PCR. Relative transcript levels (mean ± SE) were calculated from triplicate QRT-PCR reactions of independent RNA samples prepared from different batches of 3-week-old *Arabidopsis* plants. Both *WUS* and *BARD1* mRNA levels in the wild type were arbitrarily set to 1. *, $P < 0.05$ compared with the wild type.

(E) Protein gel blotting showing the presence or absence of anti-BARD1-reactive proteins in various *Arabidopsis* lines, as well an *E. coli* strain expressing a full-length ORF of *BARD1*. Lanes were loaded with total protein (20 μg) extracted from 3-week-old *Arabidopsis* lines and 10 μg total *E. coli* extract before (–) and after (+) IPTG induction. OEL, a protein sample was prepared from *BARD1* overexpressing line (*CaMV35S::BARD1*).

(F) Nuclear extracts prepared from *bard1-1*, *bard1-2* and wild-type plants retained similar ability to form a protein-DNA complex with F4 from the *WUS* promoter. Nuclear extract (10 μg) obtained from 2-week-old *bard1-1*, *bard1-2*, or wild-type plants was incubated with the DNA fragment and subjected to nondenaturing gel electrophoresis as described in Methods. –, no nuclear extract was added.

from the wild type and *bard1-1* and *bard1-2* but not from that of *bard1-3* (Figure 5E). Full-length BARD1 protein was not detected even from the *BARD1*+overexpressing line (wild-type *Arabidopsis* plants that expressed a *CaMV35S::BARD1* construct) (Figure 5E, labeled OEL). Similar protein bands were also detected using antibodies produced from a synthesized peptide. The ~80 kD protein band produced in *E. coli* only after IPTG induction was purified and subjected to matrix-assisted laser desorption/ionization time-of-flight (MALDI-TOF) identification. As shown in Supplemental Table 2 online, we obtained a total of 26 peptides corresponding to various parts of BARD1. Our results indicate that the antibody recognized BARD1 specifically. Additionally, gel shift experiments showed that the proteins produced in *bard1-1* and *bard1-2*, like the wild-type protein, retained the ability to form the BARD1-dependent protein-DNA complex (Figure 5F).

Phenotypes Similar to the *bard1-3* Mutant Are Produced in Multiple RNA Insertion Lines

Because no independent knockout lines except *bard1-3* showed severe defects in SAM organization, we generated multiple RNA interference (RNAi) lines in which the interfering RNA was targeted specifically against the last BRCT domain coding region of *BARD1*. A large number of these RNAi plants showed phenotypes similar to *bard1-3* during the early seedling stages. We photographed one such seedling (Figure 6A) and a longitudinal semithin section showing its SAM organization (Figure 6B). The

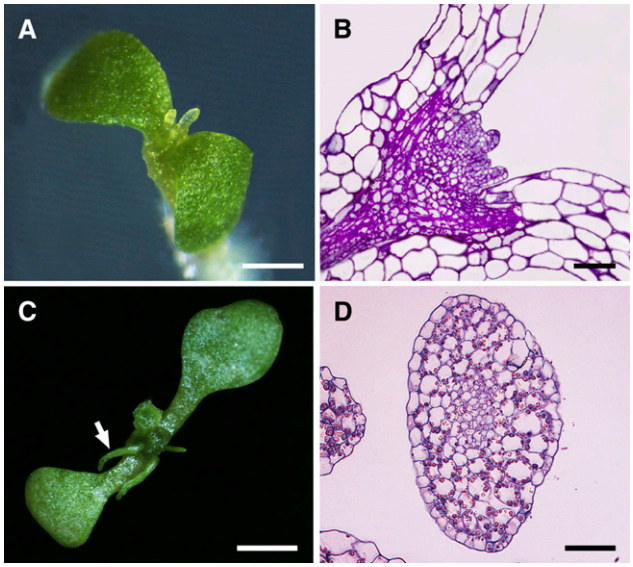

Figure 6. The Phenotype of RNAi Seedlings Expressing an RNA Directed against the Last BRCT Domain Coding Region of *BARD1* Is Similar to that of *bard1-3* Mutants.

(A) Close-up photo of a 14-d-old RNAi *Arabidopsis* seedling.
(B) Semithin longitudinal section of an RNAi seedling that was harvested at the same growth stage as in **(A)**. Note that the SAM structure is similar to that of *bard1-3* mutants.
(C) Close-up photo of a 21-d-old RNAi *Arabidopsis* seedling.
(D) Cross section of a tubular leaf-like structure observed from **(C)** (denoted by a white arrow) indicating the complete loss of leaf dorsoventrality.
White bars = 1 mm; black bars = 50 μm.

phenotype was less extreme at later stages because older seedlings produced significantly expanded, although still centric, leaf-like structures (Figures 6C and 6D). Similar to the *bard1-3* mutant plants, RNAi plants typically grew very slowly and did not go through the reproductive stage. In general, 15 to 20% of the plant lines showed phenotypes similar to those of *bard1-3*, and seedlings having the most severe growth defects were the ones that produced the lowest amounts of *BARD1* mRNA, although no quantitative analysis was performed due to limited RNA sources.

The *bard1-3* Phenotype Is Suppressed in the *wus-1* Genetic Background

The *wus-1* loss-of-function mutant was genetically crossed to *bard1-3* to obtain a homozygous *wus-1 bard1-3* double mutant *Arabidopsis* line. We used standard genotyping procedures with previously designed derived cleaved amplified polymorphic sequence primers (Wurschum et al., 2006) specific for the *wus-1* mutation and also selected for the T-DNA in *bard1-3*. The absence of functional *WUS* mRNA in this homozygous double mutant line was confirmed using a reverse primer (see Supplemental Table 1 online) derived from the mis-spliced exon 2. We sequenced the *wus-1* locus to determine the existence of the original point mutation in the homozygous double mutant. No amplification of *BARD1* mRNA was observed in the double mutant using primer pairs derived either from 5′ (1 to 485 nucleotides) or 3′ (1423 to 2145 nucleotides) regions. Loss of WUS function completely suppressed the *bard1-3* phenotype; SAM structures were identical to *wus-1* (Figures 7A to 7D). However, during the reproductive growth stage, defects were more severe in the double mutant than in *wus-1* mutants because these plants could hardly bolt and usually produced no flowers. Surprisingly, *BARD1*-overexpressing lines (*CaMV35S::BARD1*) also showed a phenotype similar to the double mutant throughout the vegetative growth stages (Figures 7E to 7H). The *bard1-3* phenotype could be complemented by genetic transformation with a genomic clone that contained the entire *BARD1* gene that included the 1.91-kb 5′ upstream and 0.7-kb downstream sequences (*BARD1*;*bard1-3*) or with a truncated version that contained the predicted smallest ORF in *bard1-1* and *bard1-2* plants (amino acids 241 to 714, BARD1:C-ter;*bard1-3*) but included the same flanking sequences (Figures 7I to 7L). Transgenic plants expressing the BARD1:C-ter;*bard1-3* construct showed obvious defects in DNA repair when compared with the wild type (see Supplemental Figure 2A online). However, much less DNA breakage (observed as TUNEL signals) was found in BARD1:C-ter;*bard1-3* seedlings than in *bard1-3* (see Supplemental Figure 2B online), indicating that the BARD1 C-terminal polypeptide may be necessary for efficient DNA repair. We were unable to produce transgenic plants that expressed the BARD1 N-terminal domain (residues 1 to 240, BARD1:N-ter;*bard1-3*).

WUS Transcript Levels Are Significantly Reduced in *CaMV35S::BARD1* Plants

Transcript analyses revealed that neither *WUS* nor *BARD1* mRNA was present (<0.003% of wild-type levels) in *wus-1 bard1-3* double mutants (Figure 8). Increased *BARD1* expression in *CaMV35S::BARD1* plants reduced *WUS* transcripts to ~25% of wild-type levels (Figure 8). These plants showed *wus-1* or *wus-1 bard1-3* double mutant–like structures. Wild-type levels of *WUS* and *BARD1* transcripts were found in *BARD1*;*bard1-3* and also in BARD1:C-ter;*bard1-3* plants (Figure 8), suggesting that BARD1 functions primarily through its C-terminal domain.

WUS May Be Regulated at the Chromosomal Structure Level

Because BARD1 can form a protein-DNA complex with roughly the same *WUS* promoter region as that bound by SYD (Kwon et al., 2005), we performed coimmunoprecipitation (co-IP) experiments to investigate a potential physical interaction between BARD1 and SYD. In vitro–expressed BARD1 was found to interact with the ATPase domain of SYD (residues 666 to 916, SYD-2-c-Myc) (see Supplemental Figure 6A online, left panel). Both BARD1-HA and SYD-2-c-Myc were coimmunoprecipitated by either anti-HA or anti-c-Myc, indicating the existence of a physical interaction between these two polypeptides (see Supplemental Figure 6A online, middle panel). However, no interaction between BARD1-HA and SYD-1-c-Myc (74.9 kD) was

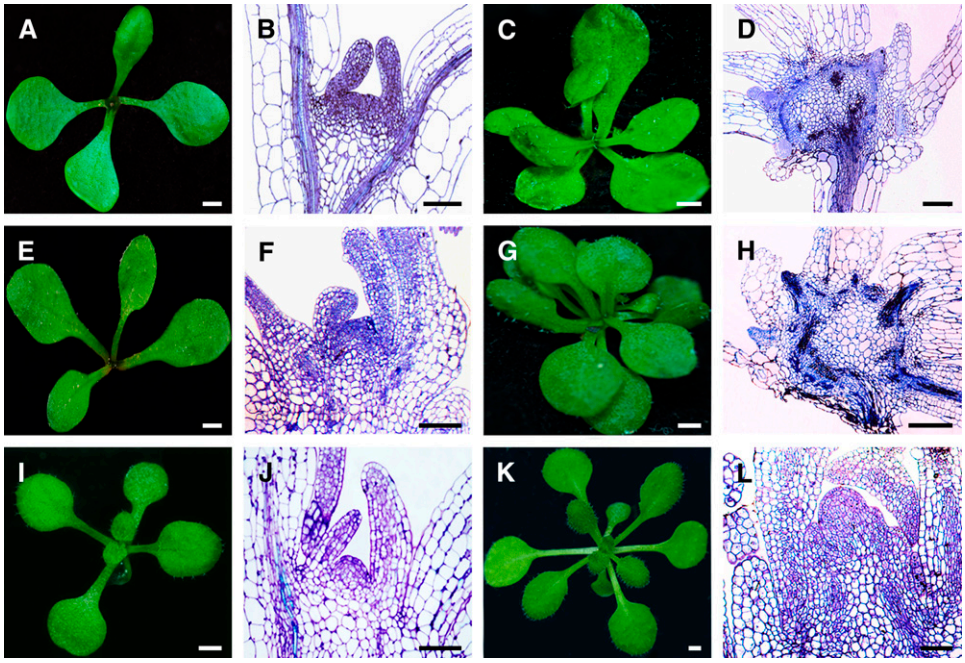

Figure 7. Comparison of Shoot Meristem Phenotypes.

(A), **(E)**, and **(I)** Photographs of 14-d-old *wus-1 bard1-3* double mutant, *CaMV35S::BARD1* (in wild-type background), and BARD1:C-ter*;bard1-3* seedlings, respectively.

(B), **(F)**, and **(J)** Median longitudinal sections of the same lines.

(C), **(G)**, and **(K)** Photographs of 25-d-old *wus-1 bard1-3*, *CaMV35S::BARD1*, and BARD1:C-ter*;bard1-3* plants, respectively.

(D), **(H)**, and **(L)** Median longitudinal sections of the same lines. White bars = 1 mm; black bars = 50 μm.

observed after co-IP: anti-HA or anti-c-Myc did not pull down the other protein present in the reaction (see Supplemental Figure 6A online, right panel). Theoretical nucleosome positioning analysis revealed that the immediate *WUS* promoter region is predicted with high probability to pack into nucleosomes (see Supplemental Figure 6B online). Furthermore, the *WUS* CAAT and TATA boxes are predicted to locate inside nucleosomes rather than being positioned in internucleosome regions, as is the case for other more ubiquitously expressed genes (see Supplemental Figures 6B and 6C online). These data indicate that substantial chromatin remodeling at or near the *WUS* promoter may be a prerequisite for *WUS* expression.

DISCUSSION

BARD1 Regulates *Arabidopsis* SAM Organization and Maintenance by Repressing *WUS* Expression

WUS activity is required for the maintenance of stem cell identity, whereas the *CLV* gene family acts to limit the size of this stem cell pool by promoting differentiation and organ primordia formation via a feedback loop that inhibits *WUS* transcription (Clark et al., 1997; Brand et al., 2000; Schoof et al., 2000; Muller et al., 2006). When the domain of *WUS* transcription was no longer confined to the OC and WUS transcript accumulated in the outermost cell layers as in *bard1-3*, cell division was promoted and organ differentiation was inhibited significantly (Figures 1L and 1P), which resulted in a multiple primordia phenotype (Figures 1K and 1O). Similarly, when *WUS* was expressed in cells that were programmed to form organ primordia under control of the *ANT* promoter, these plants could not go through seedling stages due to the accumulation of large amounts of meristem cells that failed to differentiate into organs (Schoof et al., 2000; Groß-Hardt et al., 2002). *WUS* transcripts localized outside of the OC and massive accumulation of nondifferentiated stem cells was also observed by overexpressing *POLTERGEIST LIKE1* (encoding a protein phosphatase acting downstream of the CLV signaling pathway) in a *clv* mutant background (Song et al., 2006). These results indicate that *WUS* transcription outside of the OC may be responsible for the observed *bard1-3* mutant phenotype.

Formation of the BARD1-Dependent Protein-DNA Complex May Inhibit the Chromatin Remodeling Effects of SYD

BARD1 functions as a heterodimer with BRCA1 in *Arabidopsis* (Reidt et al., 2006). Here, in vitro gel shift experiments indicated that a BARD1-dependent protein-DNA complex was formed specifically with the F4 fragment upstream of the *WUS* promoter (Figures 4C and 4D). A co-IP assay showed that SYD, a SWI2-SNF2 ATPase subunit of the chromatin remodeling complex, interacted with BARD1 (see Supplemental Figure 6A online), implying that *WUS* expression may be regulated at the

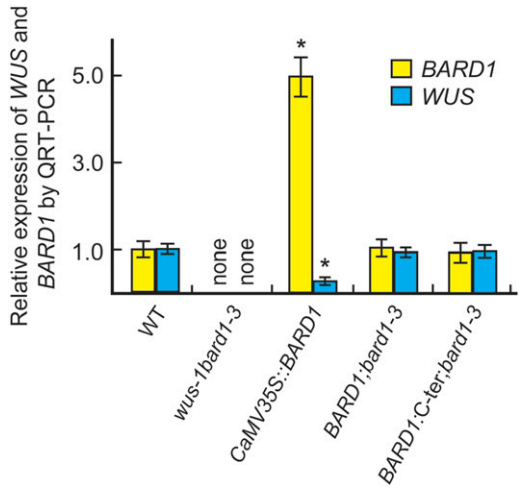

Figure 8. QRT-PCR Analysis of *BARD1* and *WUS* Expression in Different *Arabidopsis* Lines.

Quantitative analysis of *WUS* and *BARD1* transcript levels in the *wus-1 bard1-3* double mutant, *CaMV35::BARD1*, *BARD1;bard1-3*, and BARD1:C-ter*;bard1-3* seedlings, respectively. The aboveground parts of 3-week-old seedlings of the various genotypes were used for total RNA extraction, reverse transcription, and QRT-PCR analysis. Relative expression levels (mean ± SE) were calculated from triplicate independent RNA samples prepared from different batches of *Arabidopsis* plants. Levels were compared with the wild type, which was arbitrarily set to 1. "None" indicates <0.003% of wild-type *WUS* and *BARD1* transcript levels. *, $P < 0.01$ compared with the wild type.

chromosome structure level. Indeed, when chromosomal DNA sequences of the *WUS* promoter were loaded into a computational model (Segal et al., 2006), the CAAT and TATA boxes had a high probability of being buried inside nucleosomes (see Supplemental Figures 6B and 6C online); however, this was not the case when we analyzed sequences for more readily expressed genes, such as *RBCMT*, *ADH1*, *Histone H1*, and *RPL23A* (see Supplemental Figure 6C online). Thus, our data suggest that *BARD1* may repress *WUS* transcription by inhibiting the chromatin remodeling process that is, in theory, essential for *WUS* expression.

BARD1 May Repress *WUS* Expression through Its C-Terminal Domain

Analysis of *Arabidopsis bard1-1* and *bard1-2* mutant lines suggested that BARD1 is involved in DNA repair (Reidt et al., 2006). However, neither *bard1-1* nor *bard1-2* displayed the same phenotype as *bard1-3*; to address this unexpected finding, we performed 5′ RACE, which revealed that *bard1-1* and *bard1-2* plants produced 5′-truncated RNAs of 2027 nucleotides (starting from exon 3 with 19 nucleotides of intron 2 attached) and 1479 bp (starting from the middle of exon 5), respectively (Figure 5). In-frame translation start sites were found in both truncated mRNAs, indicating that these mutants might produce BARD1 C-terminal polypeptides containing functional BRCT domains important for phosphorylation-dependent protein–protein interactions (Glover et al., 2004; Narod and Foulkes, 2004; Williams et al., 2004). These truncated mRNAs in *bard1-1* and *bard1-2* were ~39 and 46%, respectively, of the wild-type mRNA level, whereas no part of the *BARD1* mRNA could be amplified from *bard1-3*. The existence of polypeptides encoded by mRNAs from *bard1-1* and *bard1-2* was confirmed by protein gel blotting experiments (Figure 5E). Our results seem to suggest that only a 52.5-kD polypeptide, but not the full-length BARD1 protein, is present in *Arabidopsis* plants. However, our data do not indicate whether the 52.5-kD form is the sole polypeptide encoded by BARD1 or the putative full-length BARD1 is cleaved in plant cells by an efficient and plant-specific protein cleavage process to produce two separate polypeptides. Also, in contrast with *bard1-3*, *WUS* mRNA in both *bard1-1* and *bard1-2* lines remained at the wild-type level, indicating that the C-terminal part of BARD1 produced in these plants was sufficient to repress *WUS* transcription, which is necessary for maintaining normal SAM organization. Indeed, homozygous transgenic *Arabidopsis* plants expressing the two C-terminal BRCT domains in the *bard1-3* background produced wild-type SAM structures (Figures 7I to 7L). These data support the hypothesis that BARD1 is essential for inhibiting *WUS* transcription outside the OC and that BARD1 functions mainly through the C-terminal BRCT domains. However, the fact that the *wus-1 bard1-3* double mutant had a more severe phenotype than *wus-1* apart from identical SAM structure suggests that BARD1 has additional effects via pathways not involving *WUS*, as reported previously (Reidt et al., 2006).

BARD1 Is Required for Proper Development of Leaf Dorsoventrality

Leaf dorsoventral polarity requires lateral information from meristem cells. Centric organs, instead of leaves with proper dorsoventrality, can be produced if the apical meristem is isolated by cutting across the apex extending from the edge of P_1 to the edge of P_2 (the two youngest leaf primordia) (Sussex, 1951). However, if the apex is only isolated from lateral information flow arising in or near P_1 and P_2, a dorsoventral leaf is produced (Sussex, 1951; Reinhardt et al., 2005). In this study, tubular-like structures, similar to those obtained by physically separating leaf primordia from developing apices, were observed on the *bard1-3* mutant (Figure 1P), indicating that BARD1 activity or a BARD1-dependent signal(s) is required for proper leaf development. Similar morphology was observed in the *Arabidopsis phabulosa-1d* (*phb-1d*) mutant and in the loss of *PHANTASTICA* (*PHAN*) *Antirrhinum* mutant (Waites and Hudson, 1995; McConnell and Barton, 1998; Hudson, 2000). Further studies are warranted to determine whether *BARD1* affects the expression pattern or the function of *PHB-1D* in *Arabidopsis* and *PHAN* in *Antirrhinum*.

In summary, our data indicate that BARD1 is essential for confining *WUS* expression to the OC and for maintaining its relative transcription level, which is vital for proper *Arabidopsis* growth and development. The identification of putative new factors involved in regulation of *WUS* expression will help elucidate the molecular mechanisms that fine-tune this master regulator.

METHODS

Plant Lines and Growth Conditions

The *Arabidopsis thaliana* plants used were mainly derived from Col-0 accessions. Three *Arabidopsis* mutant lines with disrupted *BARD1* were obtained from SALK collections (ABRC; http://signal.salk.edu): *bard1-1*, SALK_097601; *bard1-2*, SALK_031862; and *bard1-3*, SALK_003498. Seeds were surface-sterilized with 0.1% $HgCl_2$, germinated on Murashige and Skoog medium for 2 weeks, transferred to soil, and grown in fully automated growth chambers (Conviron) with a 16/8 h light/dark cycle at 23°C in 70% humidity (Wang et al., 2003). The *wus-1* mutant originated from Thomas Laux and was a gift from K. Chong.

Histological Analysis

To prepare semithin sections, seedlings harvested at different stages were fixed overnight in 2% paraformaldehyde and 2.5% glutaraldehyde in PBS, pH 7.2, on ice. Specimens were dehydrated in an ethanol series (30, 50, 70, 80, 90, 95, and 100%) and embedded in Spurr's resin (Spi-Chem) according to the manufacturer's instructions. The tissue was sectioned at a thickness of 4 μm on a Leica RM 2265 microtome (Leica). After staining with 0.05% toluidine blue, sections were observed under bright-field optics using a Leica DMR microscope.

RNA Extraction and QRT-PCR

Rosette leaves, stems, roots, and shoot apices were harvested from 3-week-old wild-type *Arabidopsis* seedlings. Radicles were prepared from *Arabidopsis* seeds 30 h after germination, flowers were collected on the day before full opening, and embryos were obtained from *Arabidopsis* siliques 1 to 4 d after anthesis. RNA extraction and QRT-PCR were performed as reported (Gong et al., 2004), 5 μg of RNAs were used for each reaction, and the housekeeping UBQ gene was used as internal standard. We used triplet replicates of independent plant samples. All primer sequences are shown in Supplemental Table 1 online. All *Arabidopsis* lines used in QRT-PCR experiments, including *wus-1 bard1-3*, *BARD1*;*bard1-3*, and *BARD1* overexpressers (*CaMV35S::BARD1*), were genotyped as reported (Wurschum et al., 2006) before being used for RNA extraction and analyses. We used the CT values method to quantify the relative amounts of target gene transcripts as reported (Xu et al., 2007).

In Situ Hybridization

In situ hybridization experiments were done as described (Mayer et al., 1998). A 696-bp fragment from the 3′ end of the *BARD1* coding region was used to generate probes using the gene-specific primers described in Supplemental Table 1 online. The full-length *WUS* coding region was used to generate the riboprobes as reported (Mayer et al., 1998). The PCR fragments were cloned into pGEM-T-easy vector (Promega) and linearized using *Nco*I or *Sal*I before being used for synthesis of 11-digoxigenin-UTP–labeled sense or antisense probes, respectively. The probes were synthesized in accordance with the manufacturer's instructions (Roche Diagnostics).

Lugol and DAPI Staining of Root Cells

For Lugol staining, 7-d-old roots were dipped in Lugol's staining solution (Sigma-Aldrich) for 3 min, washed with distilled water, and observed under a differential interference contrast microscope (Leica). For DAPI staining, *Arabidopsis* roots were fixed in 3% glutaraldehyde (Sigma-Aldrich) overnight and stained with 1% DAPI (Sigma-Aldrich) for 4 h. The roots with stained nuclei were visualized on the microscope with a UV fluorescence filter set and photographed using the Leica DFC 480 camera.

Gel Shift Assays

Oligonucleotides complementary to different motifs of the WUS promoter from −435 to −70 bp, as depicted in Figure 3A, were synthesized by Sunbiotech. The gel shift assay was performed in a total volume of 20 μL DNA binding buffer (25 mM HEPES-KOH, pH 7.5, 10% glycerol, 4 mM NaCl, 1 mM DTT, 40 mM KCl, and 0.5 mM EDTA). Nuclear extract (10 μg) prepared from wild-type or *bard1-3* mutant seedlings and 2 pmol of ^{32}P-end–labeled oligonucleotides synthesized from different DNA fragments were added to the reaction. After incubating for 2 h at room temperature, the reaction was loaded onto an 8% nondenaturing PAGE gel in 0.5× TBE (45 mM Tris-borate and 1 mM EDTA). DNA binding activity was quantified using the Typhoon 9200 PhosphorImager (GE Healthcare) as reported (Wei et al., 2005). For supershift assays, ~20 nmol of anti-BARD1 antiserum was added to the reaction after an initial 30-min incubation of the DNA fragments with nuclear extracts at room temperature. The reactions were further incubated for a total of 2 h before gel loading.

Preparation of Antiserum to BARD1

A 723-bp C-terminal part of *BARD1* was cloned into the pET-28a expression vector for protein purification using primers reported in Supplemental Table 1 online. Approximately 3 mg of proteins purified using a His-tag affinity column (Novagen) was used to immunize mice for polyclonal antibody production (performed commercially in the Antibody Center, National Institute of Biological Sciences of China). We further affinity purified the antibody using the polypeptide ELGAESSNNVNDQR (residues 639 to 652), identified by Peptide-antigen Finder (Chinese Peptide), as the affinity column tag and confirmed the quality of the antibody by an enzyme-linked immunosorbent assay before protein gel blotting analyses. A second antibody was produced from rabbit using this synthesized polypeptide as the antigen at the Antibody Center (Institute of Molecular Immunology, Peking University).

Protein Gel Blotting Analysis and MALDI-TOF Identification of BARD1

Shoots of various *Arabidopsis* plant lines were harvested, stored in liquid nitrogen, and subsequently ground into a fine powder using a mortar and pestle. Samples were homogenized in extraction buffer containing 50 mM Tris-acetate, pH 7.9, 100 mM potassium acetate, 1 mM EDTA, 1 mM DTT, 1 mM PMSF, and 20% glycerol. Cell debris was removed by centrifugation at 10,000*g* for 15 min. Immunoblotting was performed after 20 μg protein (quantified by a protein assay kit [Bio-Rad]) was subjected to SDS-PAGE (10% gel) and then transferred to a polyvinylidene difluoride membrane; purified anti-BARD1 was diluted 1:1000 in 1× PBS buffer containing 0.05% Tween 20 and 5% fat-free milk. In parallel experiments, preimmune serum was used as the negative control for antibody specificity. We also used samples extracted from one *Escherichia coli* strain carrying an expression cassette for a full-length BARD1 before and after IPTG induction to demonstrate the specificity of our antibody. This protein band was further purified and sent for MALDI-TOF identification following a previously reported procedure (Wang et al., 2006).

UV-C Treatment and Detection of in Situ Cell Death by TUNEL Assay

Wild-type and *bard1-3* mutant apical *Arabidopsis* tissues were fixed in formalin/acetic acid fixation solution, dehydrated in a series of graded ethanol, and embedded in paraffin. Sections were cut at a thickness of 10 μm using a rotary microtome (Leitz 1512). Samples were digested with 10 μg/mL proteinase K at 37°C for 30 min. UV lamps (254-nm radiation at a fluency rate of 1.0 J/m^2/s) were used to treat the plants at the indicated dosages. TUNEL assay was performed according to the manufacturer's instructions (Boehringer Mannheim) with details as reported (Li et al., 2004).

Co-IP Assay

We cloned the full-length *BARD1* downstream of the HA-tag in pGADT7 and cloned two fragments covering the N-terminal part of the SYD coding region (1 to 665 and 666 to 916, designated as SYD-1 and SYD-2, respectively; the SYD-2 fragment contained the functional ATPase domain), downstream of the cMyc-tag in pGBKT7. We used TNT-coupled wheat germ extract systems (Promega) and [^{35}S]methionine (Perkin-Elmer) for in vitro translation of the above polypeptides and performed the co-IP assay using the Matchmaker kit (Becton-Dickinson) following the manufacturer's instructions. Gels were dried and scanned using the Typhoon 9200 PhosphorImager (GE Healthcare).

Plant Transformation and Crossing

For genetic complementation of the *bard1-3* phenotype, a 6.1-kb genomic DNA that encompassed the whole *BARD1* (At1g04020) coding region plus 1.91 kb 5′ upstream and 0.7 kb downstream flanking sequences was cloned into pCAMBIA1305 using primers described in Supplemental Table 1 online. This construct was then transformed into heterozygous *bard1-3*/+ *Arabidopsis* plants. The N terminus (residues 1 to 240) or C terminus (residues 241 to 714) of BARD1 was cloned into pCAMBIA3301 that contained the same 1.91-kb *BARD1* 5′ upstream promoter and 0.7-kb downstream flanking sequences. Transgenic lines were selected by antibiotic resistance, genomic PCR, and also by cosegregation studies that looked for single-copy insertion events into the *bard1-3* homozygous background. A *BARD1* overexpression line (*CaMV35S::BARD1*) was obtained by cloning the full-length *BARD1* coding region under the *CaMV35S* promoter and the *NOS* terminator in pCAMBIA1305 and then transforming wild-type plants. Pollen collected from *wus-1* plants was used to pollinate heterozygous *bard1-3* plants to produce the homozygous *wus-1 bard1-3* double mutant.

Production of RNAi Lines

To produce transgenic plants expressing a *BARD1*-RNAi construct, a 553-nucleotide *BARD1* C-terminal coding region (1593 to 2145) was amplified using primers described in Supplemental Table 1 online and fused to the same *CaMV35S* promoter and *NOS* terminator in pCAMBIA1305, as described in the previous section. The PCR products were cloned in both sense (digested with *Sac*I and *Kpn*I) and antisense (digested with *Xba*I and *Bam*HI) directions, separated by a 10-nucleotide spacer.

Analysis of GUS Activity

p*BARD1*:*GUS* was constructed by amplifying the 1.91-kb *BARD1* promoter and inserting it between *Hin*dIII and *Xba*I sites of pBI121. GUS activity was assayed using 10-d-old seedlings, and stained tissues were processed for histological evaluation (Schoof et al., 2000; Kwon et al., 2005).

Predictions of Intrinsic Nucleosome Organization

For intrinsic nucleosome organization prediction, we used genomic sequences obtained from 2.0 kb upstream to 2.0 kb downstream of the putative transcription initiation site for *WUS* and a few readily expressed housekeeping genes and performed computational analyses using the online algorithm model obtained from yeast (Segal et al., 2006; also see http://132.77.150.113/pubs/nucleosomes06/segal06_prediction.html). For CAAT and TATA boxes analysis, promoter sequences were scanned by searching http://www.dna.affrc.go.jp/PLACE/signalscan.html.

Statistical Analysis

Statistical significance was evaluated by one-way analysis of variance followed by Tukey's test (SigmaStat 3.5; Systat Software).

Accession Numbers

Sequence data from this article can be found in the Arabidopsis Genome Initiative or GenBank/EMBL databases under the following accession numbers: *BARD1* (At1g04020, *NM_100283*), *WUS* (AT2G17950, *NM_127349*), *BRCA1* (At4g21070, *NM_118225*), and *BARD1* variant transcript in *bard1-1* (EU817406) and in *bard1-2* (EU817407).

Supplemental Data

The following materials are available in the online version of this article.

Supplemental Figure 1. Characterization of Different *bard1* Mutant Alleles.

Supplemental Figure 2. *bard1-3* Is Hypersensitive to DNA Damage.

Supplemental Figure 3. Phenotypic Characterization of the *bard1-3* Root System.

Supplemental Figure 4. RT- and QRT-PCR Analyses of Potential Target Gene Expression.

Supplemental Figure 5. GUS Expression in Transgenic *Arabidopsis* Plants Carrying the *BARD1:GUS* Construct.

Supplemental Figure 6. *BARD1* May Repress *WUS* Expression by Inhibiting the Chromatin Remodeling Process That Is Essential for *WUS* Promoter Function.

Supplemental Table 1. Primers Used for RT-, QRT-PCR, and Other Analyses.

Supplemental Table 2. MALDI-TOF Analysis of At BARD1 Expressed in *E. coli* after IPTG Induction.

ACKNOWLEDGMENT

This work was supported by grants from the National Natural Science Foundation of China (Grants 90717009 and 30221120261).

Received February 20, 2008; revised June 2, 2008; accepted June 14, 2008; published June 30, 2008.

REFERENCES

Baer, R., and Ludwig, T. (2002). The BRCA/BARD1 heterodimer, a tumor suppressor complex with ubiquitin E3 ligase activity. Curr. Opin. Genet. Dev. **12:** 86–91.

Baurle, I., and Laux, T. (2005). Regulation of *WUSCHEL* transcription in the stem cell niche of the *Arabidopsis* shoot meristem. Plant Cell **17:** 2271–2280.

Brand, U., Fletcher, J.C., Hobe, M., Meyerowitz, E.M., and Simon, R. (2000). Dependence of stem cell fate in *Arabidopsis* on a feedback loop regulated by *CLV3* activity. Science **289:** 617–619.

Brand, U., Grunewald, M., Hobe, M., and Simon, R. (2002). Regulation of *CLV3* expression by two homeobox genes in *Arabidopsis*. Plant Physiol. **129:** 565–575.

Cai, H., Tian, X., Hu, X.D., Li, S.X., Yu, D.H., and Zhu, Y.X. (2005). Combined DNA vaccines formulated either in DDA or in saline protect cattle from *Mycobacterium bovis* infection. Vaccine **23:** 3887–3895.

Clark, S.E., Williams, R.W., and Meyerowitz, E.M. (1997). The

CLAVATA1 gene encodes a putative receptor kinase that controls shoot and floral meristem size in *Arabidopsis*. Cell **89:** 575–585.

Gallois, J.L., Nora, F.R., Mizukami, Y., and Sablowski, R. (2004). WUSCHEL induces shoot stem cell activity and developmental plasticity in the root meristem. Genes Dev. **18:** 375–380.

Glover, J.N.M., Williams, R.S., and Lee, M.S. (2004). Interactions between BRCT repeats and phosphoproteins: Tangled up in two. Trends Biochem. Sci. **29:** 579–585.

Gong, W., et al. (2004). Genome-wide ORFeome cloning and analysis of *Arabidopsis* transcription factor genes. Plant Physiol. **135:** 773–782.

Groß-Hardt, R., Lenhard, M., and Laux, T. (2002). *WUSCHEL* signaling functions in interregional communication during *Arabidopsis* ovule development. Genes Dev. **16:** 1129–1138.

Hudson, A. (2000). Development of symmetry in plants. Annu. Rev. Plant Physiol. Plant Mol. Biol. **51:** 349–370.

Irminger-Finger, I., and Jefford, C.W. (2006). Is there more to BARD1 than BRCA1? Nat. Rev. Cancer **6:** 382–391.

Kieffer, M., Stern, Y., Cook, H., Clerici, E., Maulbetsch, C., Laux, T., and Davies, B. (2006). Analysis of the transcription factor WUSCHEL and its functional homologue in *Antirrhinum* reveals a potential mechanism for their roles in meristem maintenance. Plant Cell **18:** 560–573.

Kwon, C.S., Chen, C., and Wagner, D. (2005). *WUSCHEL* is a primary target for transcriptional regulation by SPLAYED in dynamic control of stem cell fate in *Arabidopsis*. Genes Dev. **19:** 992–1003.

Lafarge, S., and Montane, M.H. (2003). Characterization of *Arabidopsis thaliana* ortholog of the human breast cancer susceptibility gene 1: *AtBRCA1*, strongly induced by gamma rays. Nucleic Acids Res. **31:** 1148–1155.

Laux, T., Mayer, K.F.X., Berger, J., and Jurgens, G. (1996). The *WUSCHEL* gene is required for shoot and floral meristem integrity in *Arabidopsis*. Development **122:** 87–96.

Lenhard, M., Bohnert, A., Jurgens, G., and Laux, T. (2001). Termination of stem cell maintenance in *Arabidopsis* floral meristems by interactions between *WUSCHEL* and *AGAMOUS*. Cell **105:** 805–814.

Lenhard, M., Jurgens, G., and Laux, T. (2002). The *WUSCHEL* and *SHOOTMERISTEMLESS* genes fulfil complementary roles in *Arabidopsis* shoot meristem regulation. Development **129:** 3195–3206.

Li, J., Wang, D.Y., Li, Q., Xu, Y.J., Cui, K.M., and Zhu, Y.X. (2004). *PPF1* inhibits programmed cell death in apical meristems of both G2 pea and transgenic Arabidopsis plants possibly by delaying cytosolic Ca^{2+} elevation. Cell Calcium **35:** 71–77.

Lohmann, J.U., Hong, R.L., Hobe, M., Busch, M.A., Parcy, F., Simon, R., and Weigel, D. (2001). A molecular link between stem cell regulation and floral patterning in *Arabidopsis*. Cell **105:** 793–803.

Long, J.A., Ohno, C., Smith, Z.R., and Meyerowitz, E.M. (2006). TOPLESS regulates apical embryonic fate in *Arabidopsis*. Science **312:** 1520–1523.

Mayer, K.F.X., Schoof, H., Haecker, A., Lenhard, M., Jurgens, G., and Laux, T. (1998). Role of *WUSCHEL* in regulating stem cell fate in the *Arabidopsis* shoot meristem. Cell **95:** 805–815.

McConnell, J.R., and Barton, M.K. (1998). Leaf polarity and meristem formation in *Arabidopsis*. Development **125:** 2935–2942.

Muller, R., Borghi, L., Kwiatkowska, D., Laufs, P., and Simon, R. (2006). Dynamic and compensatory responses of *Arabidopsis* shoot and floral meristems to *CLV3* signaling. Plant Cell **18:** 1188–1198.

Narod, S.A., and Foulkes, W.D. (2004). *BRCA1* and *BRCA2*: 1994 and beyond. Nat. Rev. Cancer **4:** 665–676.

Reidt, W., Wurz, R., Wanieck, K., Chu, H.H., and Puchta, H. (2006). A homologue of the breast cancer-associated gene BARD1 is involved in DNA repair in plants. EMBO J. **25:** 4326–4337.

Reinhardt, D., Frenz, M., Mendel, T., and Kuhlemeier, C. (2005). Microsurgical and laser ablation analysis of leaf positioning and dorsoventral patterning in tomato. Development **132:** 15–26.

Sarkar, A.K., Luijten, M., Miyashima, S., Lenhard, M., Hashimoto, T., Nakajima, K., Scheres, B., Heidstra, R., and Laux, T. (2007). Conserved factors regulate signalling in *Arabidopsis thaliana* shoot and root stem cell organizers. Nature **446:** 811–814.

Schoof, H., Lenhard, M., Haecker, A., Mayer, K.F.X., Jurgens, G., and Laux, T. (2000). The stem cell population of *Arabidopsis* shoot meristems is maintained by a regulatory loop between the *CLAVATA* and *WUSCHEL* genes. Cell **100:** 635–644.

Segal, E., Fondufe-Mittendorf, Y., Chen, L., Thastrom, A., Field, Y., Moore, I.K., Wang, J.-P.Z., and Widom, J. (2006). A genomic code for nucleosome positioning. Nature **442:** 772–778.

Song, S.-k., Lee, M.M., and Clark, S.E. (2006). POL and PLL1 phosphatases are CLAVATA1 signaling intermediates required for *Arabidopsis* shoot and floral stem cells. Development **133:** 4691–4698.

Sussex, I.M. (1951). Experiments on the cause of dorsiventrality in leaves. Nature **167:** 651–652.

Tucker, M.R., and Laux, T. (2007). Connecting the paths in plant stem cell regulation. Trends Cell Biol. **17:** 403–410.

Waites, R., and Hudson, A. (1995). *Phantastica*: A gene required for dorsoventrality of leaves in *Antirrhinum majus*. Development **121:** 2143–2154.

Wang, B.C., Wang, H.Y., Feng, J.X., Meng, D.Z., Qu, L.J., and Zhu, Y.X. (2006). Post-translational modifications, but not transcriptional regulation, of major chloroplast RNA-binding proteins are related to *Arabidopsis* seedling development. Proteomics **6:** 2555–2563.

Wang, D.Y., Xu, Y.J., Li, Q., Hao, X.M., Cui, K.M., Sun, F.Z., and Zhu, Y.X. (2003). Transgenic expression of a putative calcium transporter affects the time of *Arabidopsis* flowering. Plant J. **33:** 285–292.

Wei, G., Pan, Y., Lei, J., and Zhu, Y.X. (2005). Molecular cloning, phylogenetic analysis, expressional profiling and *in vitro* studies of TINY2 from *Arabidopsis thaliana*. J. Biochem. Mol. Biol. **38:** 440–446.

Williams, R.S., Lee, M.S., Hau, D.D., and Glover, J.N.M. (2004). Structural basis of phosphopeptide recognition by the BRCT domain of BRCA1. Nat. Struct. Mol. Biol. **11:** 519–525.

Wu, L.C., Wang, Z.W., Tsan, J.T., Spillman, M.A., Phung, A., Xu, X.L., Yang, M.-C.W., Hwang, L.-Y., Bowcock, A.M., and Baer, R. (1996). Identification of a RING protein that can interact *in vivo* with the *BRCA* gene product. Nat. Genet. **14:** 430–440.

Wurschum, T., Groß-Hardt, R., and Laux, T. (2006). *APETALA2* regulates the stem cell niche in the *Arabidopsis* shoot meristem. Plant Cell **18:** 295–307.

Xu, Y., Wang, B.C., and Zhu, Y.X. (2007). Identification of proteins expressed at extremely low level in *Arabidopsis* leaves. Biochem. Biophys. Res. Commun. **358:** 808–812.

Xu, Y.Y., Wang, X.M., Li, J., Li, J.H., Wu, J.S., Walker, J.C., Xu, Z.H., and Zhong, K. (2005). Activation of the WUS gene induces ectopic initiation of floral meristems on mature stem surface in *Arabidopsis* thaliana. Plant Mol. Biol. **57:** 773–784.

Zhao, Y., Medrano, L., Ohashi, K., Fletcher, J.C., Yu, H., Sakai, H., and Meyerowitz, E.M. (2004). HANABA TARANU is a GATA transcription factor that regulates shoot apical meristem and flower development in *Arabidopsis*. Plant Cell **16:** 2586–2600.

Zimmermann, P., Hirsch-Hoffmann, M., Hennig, L., and Gruissem, W. (2004). GENEVESTIGATOR, *Arabidopsis* microarray database and analysis toolbox. Plant Physiol. **136:** 2621–2632.